Size effect in self-trapped exciton photoluminescence from SiO_2-based nanoscale materials

Yuri D. Glinka*
Institute of Atomic and Molecular Sciences, Academia Sinica, P.O. Box 23-166, Taipei 106, Taiwan
and Department of Physics and Astronomy, Vanderbilt University, Nashville, Tennessee 37235

Sheng-Hsien Lin, Lian-Pin Hwang, and Yit-Taong Chen
Institute of Atomic and Molecular Sciences, Academia Sinica, P.O. Box 23-166, Taipei 106, Taiwan
and Department of Chemistry, National Taiwan University, 1 Section 4, Roosevelt Road, Taipei 106, Taiwan

Norman H. Tolk
Department of Physics and Astronomy, Vanderbilt University, Nashville, Tennessee 37235
(Received 10 July 2000; published 8 August 2001)

Direct evidence for a size effect in self-trapped exciton (STE) photoluminescence (PL) from silica-based nanoscale materials as compared with bulk type-III fused silica is obtained. Two kinds of mesostructures were tested: (1) silica nanoparticle composites with primary particle size of 7 and 15 nm, (2) ordered and disordered mesoporous silicas with pore size ranging from ~2 to ~6 nm and wall thickness ~1 nm. The PL was induced by the two-photon absorption of focused 6.4 eV ArF laser light with intensity $\sim 10^6$ W cm^{-2} and measured in a time-resolved detection mode. Two models are applied to examine the blue shift of the STE PL (STEPL) band with decreasing size of nanometer-sized silica fragments. The first model is based on the quantum confinement effect on Mott-Wannier-type excitons developed for semiconductor nanoscale materials. However, the use of this model leads to a contradiction showing that the model is completely unusable in the case of wide-band-gap nanoscale materials (the band-gap of bulk silica $E_g \cong 11$ eV). In order to explain the experimental data, we propose a model that takes into account the laser heating of Frenkel-type free excitons (FE's). The heating effect is assumed to be due to the FE collisions with the boundary of nanometer-sized silica fragments in the presence of an intense laser field. According to the model, laser heating of FE's up to the temperature in excess of the activation energy required for the self-trapping give rise to the extremely hot STE's. Because the resulting temperature of the STE's is much higher than the lattice temperature, the cooling of STE's is dominated by the emission of lattice phonons. However, if the STE temperature comes into equilibrium with the lattice temperature, the absorption of lattice phonons becomes possible. As a result, the blue shift of the STEPL band is suggested to originate from the activation of hot (phonon-assisted) electronic transitions. Good agreement between experimental data and our FE laser heating model has been obtained.

DOI: 10.1103/PhysRevB.64.085421 PACS number(s): 81.07.−b, 78.55.Hx, 61.46.+w, 42.62.Fi

I. INTRODUCTION

The quantum confinement (QC) effect in semiconductor nanoscale materials (nanoparticles, nanoclusters, quantum dots, boxes, wires, etc.) has recently received considerable attention for its potential use in optoelectronic devices.[1] Owing to the fact that the valence-conduction band-gap increases with decreasing size of nano-objects, this effect may account for an observed shift in the excitonic photoluminescence (PL) towards higher energies in comparison with bulk materials and consequently enhances quantum efficiency.[2] The nature of the QC effect in semiconductors is quite well established.[1–3] The theory has been developed by assuming a Mott-Wannier-type of exciton (the big-radius exciton).[4,5] Thus it has become customary to explain any blue shift in the excitonic PL with decreasing nano-object size as resulting from the quantum confinement effect.

Recent studies of silica-based mesostructures such as nanoparticle composites[6] and mesoporous silicas[7] showed that the size of nanometer-sized silica fragments (nanoparticles with diameters 7–15 nm and walls among pores with thickness ~1 nm in mesoporous silicas) strongly affects the excitonic dynamics, also resulting in size-dependent PL properties. Bulk silicon dioxide (SiO_2) is a typical wide-band-gap material (the SiO_2 band-gap $E_g \cong 11$ eV).[8] Accordingly, the origin of the size effect in excitonic PL from silica-based mesostructures is expected to be different than that in semiconductor nanoscale materials because of the contribution of another exciton-type (the small-radius exciton).[8]

Since silica thin films and layers of nanometer-sized widths are extensively used in electronic devices, knowledge of the size effect on excitons in this material is of profound importance for modern solid-state physics and nanoscale technology. However, up to now only little is known regarding the origin of the size effect on excitons in wide-band-gap materials. Only one example of the quantum-size effect on the core excitons in diamond nanocrystals has been reported.[9] The nature of the core exciton in diamond (the band-gap $E_g \cong 5.5$ eV, Ref. 10) was discussed extensively and the exciton was initially assigned to the Frenkel type.[11] However, recent experimental findings point the way to the Mott-Wannier-type exciton in diamond.[12] In either case, it is characterized by a small radius (the distance between electron and hole components) ~0.17 nm (Ref. 13) although the authors of Ref. 9 used the theory developed for the big-radius Mott-Wannier excitons in order to describe the size

effect in nanodiamonds with diameter ranging from 3.5 nm to 5 μm. Alternatively, it is evident that the direct use of the theory developed on the assumption of Mott-Wannier excitons to describe the size effects in wide-band-gap nanoscale materials is inadequate. Since the small-radius exciton is associated with some atomic defects in the lattice,[14] the electron and hole components are placed at some neighboring lattice sites distanced by several angstroms (usually Frenkel-type excitons). According to the generally accepted picture in solid-state physics,[15] such excitons are able to travel throughout the crystal as a wave and is therefore responsible for energy transport. The size of nano-objects commonly studied is much larger than the distance between electron and hole components in Frenkel excitons. Hence, the QC effect on the small-radius exciton should be negligibly small even in a weak confinement regime. By contrast, an increase in excitonic energy is quite large and ranges several meV.[9] From this point of view, it is extremely important to search for other models to explain the blue shift of excitonic PL in wide-band-gap nanoscale materials, taking into account the specific features of the excitons generated.

Because an intermediate case between two main types of excitons (the Frenkel and Mott-Wannier excitons) occurs in silicon dioxide,[8] the free excitons (FE's) and self-trapped excitons (STE's) coexist in that material.[8,11] It is known that the self-trapping of FE's results from exciton-phonon coupling and appears in many insulators,[8,11] including SiO_2. According to the model of STE in SiO_2,[16] the electron component of the STE is an E' center (oxygen vacancy) and the hole is associated with a peroxy linkage ($\equiv$Si—O—O—Si$\equiv$). The self-trapping process is accompanied by a strong distortion of the SiO_2 lattice, which leads to a large Stokes shift of the STE PL (STEPL) band. The resulting intrinsic recombination in bulk silicas appears as an emission band peaked at $\sim$2.75 eV with a full width at half maximum (FWHM) of $\sim$0.7 eV and a lifetime $\tau \sim 1$ ms.[17] This emission is attributed to a triplet-to-singlet transition in STE and can be induced by ultraviolet light,[17] energetic electrons,[16] X-rays,[8] or multiphoton absorption.[6,7,18,19]

It has recently been shown[6,7] that the relaxation of FE's induced by a two-photon (TP) absorption of 6.4 eV ArF laser light in SiO_2-based nanoscale materials is very complicated. The relaxation process includes either the FE energy transfer to impurities and structural defects with a subsequent excitation of their intrinsic PL or the self-trapping of FE's followed by STE radiative deexcitation appearing as the STEPL band.[6,7] The interaction of FE's with the boundary of nanometer-sized silica fragments can occur both as an energy transfer process to the surface species (an inelastic scattering) and as an elastic scattering of FE's by the boundary, depending on the surface conditions of nanometer-sized silica fragments. We previously showed that the FE's can be laser heated up to high temperatures exceeding the activation barrier for self-trapping.[6,7] Hence, laser heating enhances the efficiency of FE penetration through the STE barrier. The situation preceding the self-trapping is also very intriguing. Because of the laser heating process, the FE energy gained from a laser field dominates over the corresponding energy losses. As a result, one can reach a high density of FE's in the silica nanometer-sized fragments resulting in the formation of biexcitons followed by nonradiative relaxation into Frenkel defects.[6] The biexcitonic model of Frenkel defect formation was suggested for bulk silica.[20,21] Hence, the study of size-dependent STEPL from silica-based nanoscale materials is essential to understand the peculiarities of FE relaxation in the confined space of nanometer-sized wide-band-gap materials.

In the current paper we present evidence for the size effect in STEPL from silica-based nanoscale materials induced by TP absorption of 6.4 eV ArF laser light. The PL measurements were performed with the two kinds of mesostructures: silica nanoparticle composites and recently discovered mesoporous silicas.[22] The blue shift of the STEPL band observed in the nanoscale materials with respect to the corresponding band in bulk silica has been analyzed by two models. One of them takes into account the QC effect on Mott-Wannier excitons typically occurring in semiconductor nanomaterials. However, the use of this model leads to a contradiction showing that the model is completely unusable when it is applied to small-radius excitons. We propose a model, which is based on the conception of laser heating of Frenkel-type FE's. In this case exciton heating is due to collisions with the boundary of the confined regions of nanometer-sized silica fragments in the presence of an intense laser field. According to the model, the FE laser heating increases the efficiency of the STE barrier penetration, giving rise to extremely hot STE's. As a result, the blue shift of the STEPL band is proposed to originate from the activation of hot (phonon-assisted) electronic transitions. Our treatment of the experimental data by the two models unambiguously shows that in some cases the blue shift of PL bands in wide-band-gap nanoscale materials cannot arise from the QC effect but instead results from many-body FE dynamics involving the FE heating effect. These results are expected to be useful in order to avoid errors in the interpretation of size-dependent properties of wide-band-gap nanoscale materials in general.

II. EXPERIMENTAL SECTION

A. Materials

Two kinds of variously sized silica nanoparticles (Aerosil, Degussa) and three kinds of mesoporous silicas of different pore size in comparison with type-III fused silica as a bulk material were studied. According to the vendors specification, the commercially available silica nanoparticles of a specific surface area 300 and 160 m^2/g have the nominal particle size of 7 and 15 nm (diameter), respectively.[23] The bulk silica measured contains a large concentration of hydrogen-related species,[24] hence it is close in properties to the powders used.[6,7,19,23] Mesoporous silicas were synthesized using the method described previously,[7] which is similar to that originally proposed.[22] The solids obtained have been examined by the powder x-ray diffraction method. On the basis of x-ray diffraction patterns and previous data,[7,22,25,26] we have concluded that the sample with d_{100} spacing (repeat distance) of 3.83 nm is characterized by a crystalline ordering, thus it corresponds to the MCM-41 material.[22] By contrast, the samples with d_{100} spacings of 2.9 and 7.1 nm are suggested

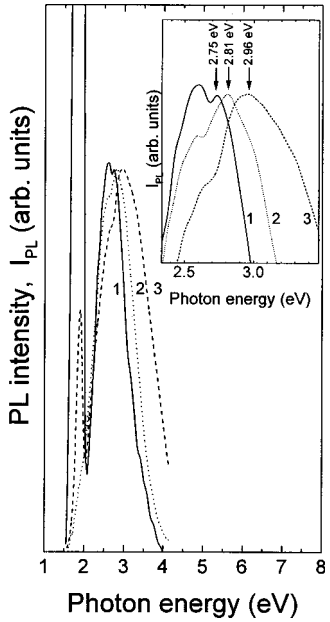

FIG. 1. Normalized time-resolved PL spectra for type-III fused silica (1) and silica nanoparticles with the size of 15 (2) and 7 nm (3) at 90 K and $\lambda_{exc}=193$ nm ($I_L=1.15$ MW/cm^2). Inset shows the same PL spectra on an enlarged scale. The spectra were detected with the following gate-delay/gate-width ratios in microseconds: 10/1 (1), 0/0.05 (2, 3).

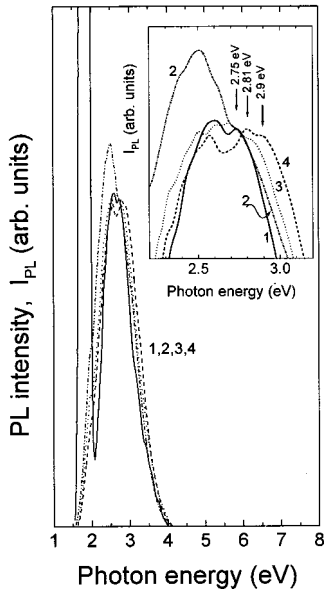

FIG. 2. Normalized time-resolved PL spectra for type-III fused silica (1) and mesoporous silicas with the pore size of ~3 (2), ~2 (3), and ~6 nm (4) at 90 K and $\lambda_{exc}=193$ nm ($I_L=1.15$ MW/cm^2). The spectrum (2) corresponds to the ordered material (MCM-41), whereas (3) and (4) represent the disordered ones. Inset shows the same PL spectra on an enlarged scale. The spectra were detected with the following gate-delay/gate-width ratios in microseconds: 10/1 (1), 0/0.05 (2–4).

to be amorphous.[7,22,25,26] Note that the hexagonal pores of disordered materials are not an ordered regular array as occur in MCM-41 despite the fact that all remaining properties are very similar.[22] It is known that the d_{100} spacings actually reflect the pore size, neglecting the wall thickness (~1 nm).[27] Therefore we approximately estimate the pore size of materials as ~3, ~2, and ~6 nm, respectively. All powders used were pressed into pellets and then heat pretreated at $T_{ht}=1173$ K for 2 h in air. The samples were placed into a vacuum chamber immediately after the heat pretreatment procedure.

B. PL measurements

PL measurements were performed in a vacuum chamber at 90 K using an ArF pulsed laser [$\lambda_{exc}=193$ mm(20 ns); Lumonics, EX-742] with a repetition rate of 10 Hz as a source of excitation. The laser beam was focused by a 30 cm lens into a 0.03 cm^2 spot. The intensity of laser light could be varied by a set of quartz plates and has been controlled to be enough to initiate the TP adsorption process.[6,7] No specimen damage was observed during laser light irradiation in the applied range of intensities. The specimens were oriented to the laser beam by 45°. The PL was collected in a conventional 90° geometry by 0.5 m SpectraPro-500 monochromator (Acton Research Corporation) with 1200 grooves/mm grating blazed for the 500 nm. The PL spectra were recorded in a time-resolved detection mode by using an R943-02 photomultiplier (peak wavelength 300–800 nm, Hamamatsu) connected with a gated electronic system (SRS-250, Stanford Research System). A set of optical filters has been used in order to cut scattered laser light from specimens. A LeCroy oscilloscope was used to measure the PL time decay constants.

III. RESULTS AND DISCUSSION

A. Experimental results

The time-resolved PL spectra from silica nanoparticles and mesoporous silicas measured with ArF laser excitation ($\lambda_{exc}=193$ nm) are shown in Figs. 1 and 2, respectively. The spectra were compared with that of type-III fused silica used as a corresponding bulk material. Overall, the PL spectra consist of three contributions located in the red, green, and blue spectral ranges in good agreement with previous data.[6,7,23] Because the assignment of the PL bands measured in the conventional detection mode was done previously,[6,7,23] we do not consider it here in detail. Note only that the green band peaked at ~2.37 eV is characterized by a progression with an origin (0-0 transition) at about 2.50 eV for 15 nm particles and about 2.55 eV for 7 nm ones.[6] This band has been assigned to hydrogen-related species.[6,7,23] The band located in the red spectral range and peaked at 1.91 eV results from the nonbridging oxygen hole centers (NBOHC's).[6,7,19,23,28,29] The blue band is attributed to emission from STE's (see Ref. 6 and references therein) and is our main interest here. The assignment of the blue band is based on the fact that the emission can only be induced when TP regime of PL excitation has been used. Also, the blue band gradually disappears with decreasing laser light intensity despite the fact that green and red bands remain strong,

indicating a decrease in the efficiency of the STE barrier penetration owing to the lack of FE laser heating.[6] Note that the spectra presented in Figs. 1 and 2 were measured with the appropriate gate-delay/gate-width parameters, at which the blue PL band appears with maximal intensity.

It has been shown recently that the laser light intensity dependences of the PL yields for these PL bands can be either quadratic or linear depending on the surface condition of nanometer-sized silica fragments.[6,7] The proposed reason for that is the existence of several pathways in the TP-produced FE relaxation.[6,7] Accordingly, an indirect excitation of green- and red-light emitters can occur. This mechanism involves the radiationless FE energy transfer into hydrogen-related species and NBOHC's followed by excitation of their intrinsic electronic transitions and subsequent light emission. An alternative pathway in the FE energy relaxation is related to the self-trapping process. The further STE radiative relaxation leads to light emission appearing as the STEPL band.

The blue band in type-III fused silica measured is peaked at 2.75 eV with FWHM and a time-decay constant in good agreement with previous data.[17] However, the STEPL band is blue shifted in silica-based mesostructures (Figs. 1 and 2) despite the fact that the green and red bands occur at the same position as for bulk silica. It can be easily seen that the green band in time-resolved spectra is peaked in the range corresponding to the origin of green band progression (2.5–2.55 eV). This fact indicates that the green band appears as a weak-intensity shoulder, so it does not affect dramatically the STEPL peak. Therefore, we estimate the peak position of the STEPL band as a maximum in the blue PL band appearing in spectra. The exact identification of the energies of the STEPL peak is shown in Figs. 1 and 2 by arrows. The greatest shift of STEPL band (~0.21 eV) with respect to the corresponding band for bulk silica was observed for the 7 nm particles. The shift for the 15 nm particles is ~0.06 eV. Note that the resulting 2.81 and 2.96 eV bands are characterized by a larger FWHM (~0.8 and 1 eV, respectively) and decay much faster ($\tau \sim 4-5\ \mu$s at 90 K). The more rapid decay of the STEPL in comparison with those typically observed for bulk SiO_2 materials is interpreted as an increase in the self-trapping efficiency for FE's owing to their laser heating.[6,7]

Analogously, the STEPL band is shifted towards the higher energies for disordered mesoporous silicas (Fig. 2). At the same time, the band shows little or no shift in the case of ordered MCM-41. Our sophisticated treatment of the PL spectra allows one to assume that the blue shift originates from the rise of additional emission components for the STEPL band. Since the components arise at the short-wavelength side, it appears as a blue shift of the STEPL band as a whole. It can be easily seen that only a single additional component peaked at ~2.81 eV arises in the case of smaller pore sized (2 nm) material (Fig. 2, curve 3). One can observe two additional components peaked at ~2.81 and ~2.9 eV for the 6 nm pore sized mesoporous silica (Fig. 2, curve 4). Hence, the shifts of STEPL band for mesoporous silicas with respect to the corresponding band for bulk silica are ~0.06 eV for the 2 nm pore sized material and ~0.06 and ~0.15 eV in the case of 6 nm pore size. Because the exact size of silica fragments (the wall thickness) in mesoporous materials is difficult to estimate, we are not able to associate directly the greater blue shift with the smaller wall thickness. However, we will show later that this statement is quite correct, so the wall thickness in larger pore sized materials is expected to be thinner than that for smaller pore size.

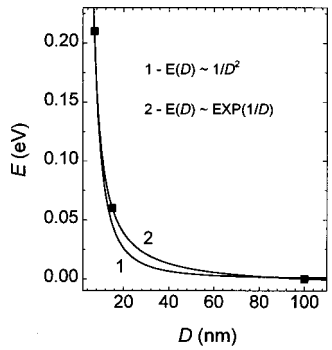

FIG. 3. The blue shift of STEPL peak plotted against the primary size of silica nanoparticles (black squared points); the point corresponding to type-III fused silica is marked as a 100-nm-sized particle. The fit to the data by $1/D^2$ and $\exp(1/D)$ function types are drawn by solid lines marked as (1) and (2), respectively.

The following sections discuss the nature of the blue shift occurring for the STEPL band taking into account two different models based on the QC and FE laser heating effects. We will restrict our consideration to the model of spherical silica nanoparticles despite the fact that the conclusions made can be applied to the silica-based mesostructures as a whole.

B. The quantum confinement effect treatment

Let us analyze the experimental results presented in the preceding section from the QC effect standpoint. As we mentioned above, the theory of QC effect has been developed for semiconductor nanoscale materials on the assumption of Mott-Wannier-type excitons.[4,5] The energy of excitons in semiconductors rises with decreasing size of nanoparticles as

$$E(D) = \frac{2\hbar^2\pi^2}{m^*_{e\text{-}h}D^2}, \tag{1}$$

where the efective mass of the exciton $m^*_{e\text{-}h}$ taken as either

$$m^*_{e\text{-}h} = m^*_e + m^*_h \quad \text{or} \quad m^*_{e\text{-}h} = \frac{m^*_e m^*_h}{m^*_e + m^*_h} \tag{2}$$

corresponds to weak and strong QC regimes, respectively. Here $E(D)$ is measured from the minimum excitonic energy corresponding to bulk materials, D is the nanoparticle diameter and m^*_e and m^*_h are effective electron and hole masses. Alternatively, two QC regimes reflect the ratio of nanoparticle size D to the effective bohr radius a^*_b of the exciton in bulk materials.[5] As this takes place, two limiting cases, $a^*_b \ll D$ and $a^*_b \gg D$, correspond to the weak and strong QC regimes, respectively. According to this theory, we have treated the blue shift of the STEPL band in silica nanoparticles by Eq. (1). The result of a fit to the data is shown as a solid line in Fig. 3 (curve 1). From this fit we obtain the

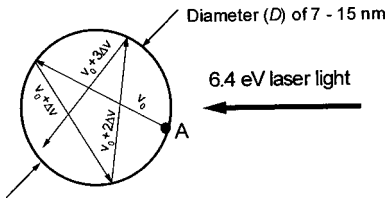

FIG. 4. SiO_2 nanoparticle exposed to 6.4 eV laser light. It is assumed that the FE could be generated at the point A.

value of $m^*_{e\text{-}h}=1.31\times10^{-31}$ kg. According to the experimentally obtained fact that in silica glasses $m^*_e=m^*_h\cong m$,[30] where $m=9.11\times10^{-31}$ kg is the electron mass, one can get using Eq. (2) the following values for $m^*_{e\text{-}h}=18.22\times10^{-31}$ and 4.56×10^{-31} kg for the weak and strong QC, respectively. Because the value of $m^*_{e\text{-}h}$ obtained from the fit is smaller than that required for strong QC, one can conclude that the strong QC regime is more appropriate to occur in silica nanoparticles. However, since the effective bohr radius a^*_b of STE in SiO_2 is estimated to be $\sim$0.5 nm (Ref. 30) and the minimal diameter of nanoparticles used $D=7$ nm, it is reasonable to expect a weak QC regime. This contradiction reflects a limit in the theory developed for the Mott-Wannier excitons in semiconductors to describe the size effect in STEPL from wide-band-gap nanoscale materials. In other words, the experimentally observed blue shifts are extraordinarily large compared to that expected from the theory.

The STEPL measurements for mesoporous silicas support this statement as well. It is known that the wall thickness in ordered and disordered mesoporous silicas is estimated to be $\sim$1 nm.[27] Evidently, since this value is much smaller than the minimal diameter of nanoparticles used, it is reasonable to expect that the blue shift should be greater than that for the 7 nm silica particles. However, the band shift observed is smaller, indicating again some contradiction with the theory. Finally we note that all experimental results discussed show that the nature of the size effect in STEPL from silica-based nanoscales is different from that occurred in semiconductor nanoscale materials.

C. The FE laser-heating effect treatment

1. Setting up the problem

Now we present an alternative model based on the conception of FE laser heating to explain the size effect in STEPL from silica-based mesostructures (Figs. 4 and 5). It is well known that the self-trapping process is caused by a localization of FE's in the lattice, which requires excitonic energy reduction.[11] As a result, the STE states occur below the FE ones (Fig. 5). It is predicted that there exists a STE barrier for FE's which can be passed either by tunneling or by activation (Fig. 5).[11] We previously showed that the FE heating up to energy exceeding the activation barrier enhances their efficiency to be self-trapped.[6] By contrast, the cooled FE's are able to reach STE states only by tunneling. Totally, the efficiency of the FE penetration through the STE barrier increases with the FE temperature (kinetic energy) and reaches its maximum when the FE energy exceeds the activation energy required for overcoming the barrier. Because extremely hot STE's occur after the FE passes through the STE barrier, the thermalization of STE's is dominated by the emission of lattice phonons (the cooling of STE's and heating of nanometer-sized silica fragments). However, if an equilibrium condition is achieved between the electron-hole and lattice-phonon subsystems, the STE is able either to emit or absorb phonons. The activation of hot (phonon-assisted) electronic transitions can occur at the aforesaid equilibrium condition.

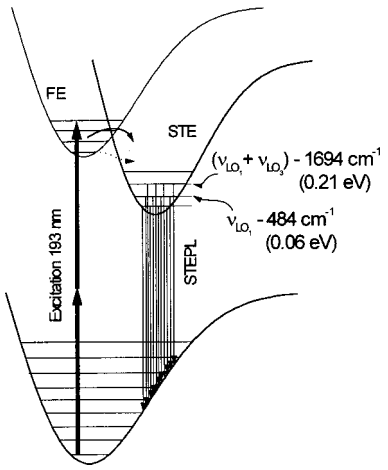

FIG. 5. Schematic diagram in the terms of chemical bonding in ≡Si—O—Si≡ clusters for FE's and STE's in silica and corresponding absorption and emission transitions. The solid and dashed arrows show two possibilities for the self-trapping barrier overcome by activation or by tunneling, respectively. The hot transitions (phonon-assisted) are shown additionally.

It has been recently established that the main specific feature of the laser heating process for TP-produced FE's generated in the confined space of silica-based nanoscale materials is the fact that the FE's are produced at the condition when intense laser light is applied ($\sim10^6$ W cm^{-2}).[6] This results from the fact that the rate of TP transitions is usually small,[31] so the laser light used should be much stronger in order to reach an excitation than that required for the single-photon process. Additionally, the mean free path length, L, for FE in bulk silicas is much longer than the size of silica fragments in mesostructures considered (for example, in type-III fused silica $L\sim500$ nm).[8] The latter feature indicates that FE's should suffer collisions with the boundary of confined regions. It has been recently shown[6,7] that the interaction of FE's with the boundary can occur either as the FE energy transfer into the surface species with subsequent light emission or without energy transfer as an elastic scattering (Fig. 4). Of course, an FE collision with the nanoparticle boundary should be considered as an interaction with some surface atom. However, we will continue to refer to the process as an interaction with the nanoparticle boundary bearing in mind the FE scattering by surface atoms. Taking into account this assumption, one can predict that a FE is able to suffer many collisions with the boundary within the applied laser pulse. As this takes place, the frequency of collisions will tend to be higher with decreasing size of silica fragments. Under these conditions the FE's can additionally gain

energy from a laser field and be heated up to high temperature, creating an electron-hole plasma. We have recently proposed that the TP-excited PL from silica-based mesostructures reflects the dynamics of FE relaxation in the confined space of nanometer-sized silica fragments, including either elastic or inelastic scattering by the boundary, the laser heating of FE's resulting in an increase in the self-trapping rate and the formation of biexcitons relaxing into Frenkel defects.[6,7]

Note that the FE cannot directly gain additional energy from the laser field, similarly as free electron in an ionized plasma.[32–34] It can be shown that if we assume that such a process occurs, then the conservation rules for energy and momentum cannot be satisfied simultaneously.[34] However, this is not the case for FE's suffering collisions with the boundary in a similar way as for electron-ion collisions in plasma[32–34] and on the surface of silica nanoparticles.[35] At the stated conditions the FE's are able to gain additional energy from an electromagnetic field. Accordingly, their maximal kinetic energy $E_{e\text{-}h}$ can be expressed as follows[34,35]

$$E_{e\text{-}h}=E_{\mathrm{ini}}+E_{\max}, \tag{3}$$

where E_{ini} is an initial energy of FE's after their generation and $E_{\max}$ is the greatest possible energy of FE's gained within the laser heating process,

$$E_{\max}=\sum_{n=1}^{\kappa}\Delta E^{(n)}=\kappa\Delta E^{(n)}, \tag{4}$$

where κ is the maximal number of collisions within the laser pulse duration of τ_L, and $\Delta E^{(n)}$ denotes the energy increment due to a single collision, which corresponds to an increment of the FE velocity ΔV (Fig. 4). The energy increment $\Delta E^{(n)}$ can be found similarly as for electron laser heating in an ionized plasma.[34] According to Eq. (4), the greatest possible energy of FE's is determined by the energy increment due to a single collision and the maximal number of FE collisions with the nanoparticle boundary within the laser pulse duration of τ_L. Evidently, the collision number depends on the mean free path length of FE between two sequential collisions, which in turn is determined by the diameter of nanoparticles. All these issues will be considered in the next sections. However, because to our knowledge the FE laser heating process in nanoscale solids has never been considered before, let us first summarize briefly the solid-state background required to solve the problem.

2. The solid-state background of the FE laser heating problem

The picture suggested in general resembles the behavior of electrons suffering collisions with ions in an ionized plasma.[32–34] To clarify this statement we briefly recall several known propositions from solid-state physics providing the basis, on which the FE laser heating problem could be solved. It is known that the electron in the solid state can be considered as a quasiparticle.[14,15] Slater suggested a procedure to average the exchange interaction of quasiparticles in the solid state, which is responsible for the modification of the Hartree-Fock equation for electron gas into the one-electron Schrödinger's equation for the solid state:[14]

$$\left\{-\frac{\hbar^2}{2m}\Delta+V(r)-e\int\frac{\rho(r')-\overline{\rho}^{\mathrm{HF}}(r,r')}{|r-r'|}d\tau'\right\}\varphi_j(r)=E_j\varphi_j(r), \tag{5}$$

where $\overline{\rho}^{\mathrm{HF}}(r,r')$ is Slater's averaging of the exchange interaction of $[\rho_j^{\mathrm{HF}}(r,r')]$ in the Hartree-Fock equation, and $\varphi_j(r)$ are Bloch functions as one-electron functions in the Slater determinant.[14] Since the whole Hamiltonian of interaction in Eq. (5) after Slater's averaging does not depend on j, it is common to all electrons of the system. According to this approximation, the electrons in the solid can be considered as noninteracting quasiparticles propelled by some total averaged potential [second and third terms in Eq. (5)]. As this takes place, the quasifree electron is characterized by the mean electron velocity, the mean electron momentum, and the effective mass. Finally, the electron motion in the solid state is equivalent to a motion of quasiparticle with the effective mass m_e^* in a viscous state with the friction coefficient of $1/\tau$, where τ is the relaxation time.[14] We will use the previously mentioned solid-state background to describe the behavior of FE's in the confined space of the nanometer-sized silica fragments of silica-based mesostructures. Despite the fact that the FE's in the solid should be considered as quasifree excitons, we will continue to use the term FE's bearing in mind quasiparticles. Note also that in the general case it is necessary to solve the Boltzmann equation, describing the FE relaxation in the solid state due to interaction with optical phonons.[14] However, because the mean free path length of FE's in bulk silica is much longer than the size of silica fragments in mesostructures considered, the relaxation time τ among collisions with the boundary of confined regions is negligibly small. At the condition mentioned the kinetic energy of FE's will be affected exclusively by the interaction with the boundary rather than the interaction with optical phonons. As a result, we can neglect all the processes of energy dissipation for FE's due to interaction with phonons and consider thereof as the free quasiparticles of effective mass $m_{e\text{-}h}^*$ interacting with the nanoparticle boundary. Moreover, we assume that the FE energy gained by collisions is much greater than that initially taken at FE generation. This statement corresponds to the condition, at which the increment of FE velocity due to each collision with the boundary should be much higher than the initial velocity of FE's, $\Delta V\gg V_0$. Really, the initial kinetic energy of FE's can be estimated as follows

$$E_{e\text{-}h}=2\hbar\omega_{\mathrm{exc}}-E_g-(E_g\text{-}E_{g_x})-E_A-\langle\hbar\omega_{\mathrm{LO}}\rangle\approx 0.8\,\mathrm{eV}, \tag{6}$$

where $\hbar\omega_{\mathrm{exc}}=6.4$ eV is the laser photon energy, $(E_g-E_{g_x})$ is the FE binding energy, where E_{g_x} denotes the FE energy gap (~10.2 eV),[8] E_A is the activation energy for FE hopping (~0.1 eV, Ref. 8) and $\langle\hbar\omega_{\mathrm{LO}}\rangle$ denotes the average energy of LO phonons in silica nanoparticles (~0.1 eV).[36] Since the value estimated is much smaller than the energy of laser photons used and which could be additionally absorbed

within the FE laser heating process, we will neglect the initial energy of FE's taken without collisions. Then Eq. (3) with Eq. (4) can be rewritten as

$$E_{e\text{-}h}=\kappa\Delta E^{(n)}=\frac{\kappa m^*_{e\text{-}h}(\Delta V)^2}{2}. \tag{7}$$

Note that the notions of the FE mean-free-path length and FE lifetime commonly used for bulk materials lose completely their meaning under the conditions mentioned because of the lack of energy dissipation of FE's among collisions. The lifetime of FE's in this case is determined exclusively by the pulse duration of laser light. Accordingly, the total average effective mean-free-path length of FE's will be determined as $L=\Sigma_{n=1}^{\kappa}\langle L_{\rm eff}^{(n)}\rangle$, where $\langle L_{\rm eff}^{(n)}\rangle$ is the average effective mean-free-path length of the FE between two sequential collisions. The word ''effective'' reflects the limited utility of the notion of the FE mean free path length in the case of nanometer-sized solids.

3. Laser heating of the plasma

In the current section we briefly consider the laser heating of electrons in an ionized plasma as an analog of the process occurring with FE's in silica-based nanoscale materials. The electron heating by electromagnetic waves is well known, and is usually referred to the inverse bremsstrahlung process.[32–34] This process is associated with the absorption of additional quanta from the laser field due to electron scattering in the presence of a strong electromagnetic wave. The additional energy can be gained either by single-photon absorption or by a multiphoton process depending on the intensity and frequency of laser light.[32–34] Accordingly, the energy rate equation for an electron in ionized plasma in the presence of an intense laser field of amplitude E_0 is expressed as follows[34]

$$\frac{dE}{dt}=\frac{e^2E_0^2\nu}{2m(\omega^2+\nu^2)}-\frac{2Em\nu}{M}, \tag{8}$$

where the first term describes the energy gain and the second one corresponds to the energy loss due to collisions with ions. In Eq. (8) e and m are the electron charge and mass, M is the ion mass, and ω and ν denote the frequencies of the laser field and collisions, respectively. The direct integration within the laser pulse duration of τ_L and using the initial condition $E=0$ when $t=0$ gives

$$E=\frac{Me^2E_0^2}{4m^2(\omega^2+\nu^2)}\left[1-\exp\left(-\frac{2m\nu\tau_L}{M}\right)\right]$$
$$\approx\frac{e^2E_0^2\nu\tau_L}{2m(\omega^2+\nu^2)}=\frac{\lambda^2r_eI_L\nu\tau_L}{\pi c(1+\nu^2/\omega^2)}\approx\frac{\lambda^2r_eI_L\nu\tau_L}{\pi c}, \tag{9}$$

where it has been reasonably assumed that $M\gg m$ and $\omega\gg\nu$, also taken into account that the laser light intensity is $I_L=(c/8\pi)E_0^2$, $\lambda=2\pi c/\omega$ is the laser light wavelength, $r_e=e^2/mc^2$ is the classical electron radius, and c denotes the velocity of light in vacuum. It can be easily seen that the energy gained by the electron linearly depends on the laser light intensity indicating the single-photon inverse bremsstrahlung process. One can show that in the case of a nonlinear interaction the efficiency of light absorption will depend on the intensity in power α, where α denotes the number of photons taking part in the absorption process.[32–34]

4. The energy gained by FE due to a single collision with a nanoparticle boundary

According to the previous discussion, Eq. (9) could be applied to a free electron in the solid with m_e^* in place of m. Then the classical electron radius r_e is transformed into the polaron radius $r_p=e^2/\varepsilon m_e^*c_m^2$, where ε and c_m are the dielectric constant and the velocity of light in a medium, respectively.[11] In a similar way the substitution of m_h^* into Eq. (9) gives the expression describing the energy gain for holes with the same polaron radius r_p, because of $m_e^*=m_h^*\equiv m$.[30] The energy gained by each collision is equal in magnitude because all the parameters discussed are constant at the fixed intensity of laser light used. The effective laser field in a medium increases by the factor of $E_{\rm eff}=E_0+(4\pi/3)P$, where P is the total polarization of a medium, which in the high-frequency limit is expressed as $P=(\varepsilon_\infty-1)E_0/4\pi$,[14] where ε_∞ is the high-frequency dielectric constant (for silica $\varepsilon_\infty=2.14$, Ref. 36). Finally, the FE energy gain due to a single nth collision with the nanoparticle boundary can be expressed as a sum of energies gained by electron and hole together. Then we have

$$\Delta E^{(n)}=\frac{m^*_{e\text{-}h}(\Delta V)^2}{2}\approx\frac{2\lambda^2r_pI_L^{\rm eff}}{\pi c_m}, \tag{10}$$

where $I_L^{\rm eff}=(c_m/8\pi)E_{\rm eff}^2$ is the effective laser light intensity in nanometer-sized silica fragments. Here we used the collision number within τ_L as $\kappa=\nu\tau_L=1$. Correspondingly, the increment of the FE velocity due to an nth collision is

$$\Delta V\approx\left(\frac{4\lambda^2r_pI_L^{\rm eff}}{m^*_{e\text{-}h}\pi c_m}\right)^{1/2} \tag{11}$$

Note that we do not consider here the nonlinear FE laser heating because such processes are expected to occur only at laser light intensities much higher than used in our measurements.

5. The average effective mean-free-path length between two sequential collisions

In this section we consider the effective mean-free-path length of FE's suffering collisions with the nanoparticle boundary. Because the FE is assumed to be involved in an elastic scattering process, it may be scattered by the boundary in an arbitrary direction inside nanoparticle. Note that such a situation repeats for each collision and the total path length of the FE within a time frame of τ_L is determined as a sum of effective mean-free-path lengths between all sequential collisions. It is easy to show taking into account the differential area element on the surface of a spherical shell with diameter D, that the probability of FE scattering by the boundary over a whole set of directions, making an angle

between ϑ and $\vartheta + d\vartheta$ with respect to a tangent plane to the surface is $dW = \cos\vartheta\, d\vartheta$. Then the average effective mean-free-path length for nth collision is found by standard procedure

$$\langle L_{\text{eff}}^{(n)} \rangle = \int l\, dW = \int_0^{\pi/2} l \cos\vartheta\, d\vartheta, \tag{12}$$

where $l = D \sin\vartheta$ is a chord. Finally, the integration yields

$$\langle L_{\text{eff}}^{(n)} \rangle = \int_0^{\pi/2} D \sin\vartheta \cos\vartheta\, d\vartheta = D/2. \tag{13}$$

Therefore, the total average effective mean-free-path length of the FE, suffering κ collisions within a time frame of τ_L, is $L = \Sigma_{n=1}^{\kappa} \langle L_{\text{eff}}^{(n)} \rangle = \kappa D/2$.

6. The maximal number of FE collisions in a nanoparticle of diameter D within τ_L

According to previous sections, the FE moves uniformly through the nanoparticle body among collisions with the initial velocity of V_0. After each collision with the boundary, the energy of FE's increases by the value of $\Delta E^{(n)}$, which corresponds to an increase in the velocity of the FE by ΔV (Fig. 4). Using this model, the time required for the FE to reach the boundary for the first time is expressed as $\Delta t_0 = \langle L_{\text{eff}}^{(n)} \rangle / V_0$. The time between first and second collisions is $\Delta t_1 = \langle L_{\text{eff}}^{(n)} \rangle / (V_0 + \Delta V)$. Correspondingly, the time between $\kappa - 1$ and κ sequential collisions is $\Delta t_\kappa = \langle L_{\text{eff}}^{(n)} \rangle / (V_0 + \kappa \Delta V)$ (Fig. 4). It is evident that in the framework of the model considered $\Sigma_{i=0}^{\kappa} \Delta t_i = \tau_L$. Hence we can write

$$\tau_L = \frac{\langle L_{\text{eff}}^{(n)} \rangle}{\Delta V} \left(\frac{\Delta V}{V_0} + \frac{1}{\frac{V_0}{\Delta V} + 1} + \frac{1}{\frac{V_0}{\Delta V} + 2} + \frac{1}{\frac{V_0}{\Delta V} + 3} + \cdots + \frac{1}{\frac{V_0}{\Delta V} + \kappa} \right). \tag{14}$$

Because we use again approximation $\Delta V \gg V_0$, the $\Delta V / V_0$ terms in the denominators of series can be left out. Then we have

$$\tau_L = \frac{\langle I_{\text{eff}}^{(n)} \rangle}{\Delta V} \left(\frac{\Delta V}{V_0} + 1 + \frac{1}{2} + \frac{1}{3} + \cdots + \frac{1}{\kappa} \right). \tag{15}$$

When working with such a type of series we recognize the Euler's constant $\gamma = 0.577\ldots$ (Ref. 37) and

$$\gamma = \lim_{n \to \infty} \left(1 + \frac{1}{2} + \frac{1}{3} + \cdots + \frac{1}{n} - \ln n \right). \tag{16}$$

Hence,

$$\gamma + \lim_{n \to \kappa} \ln n = \lim_{n \to \kappa} \left(1 + \frac{1}{2} + \frac{1}{3} + \cdots + \frac{1}{n} \right). \tag{17}$$

Then Eq. (15) can be rewritten as follows

$$\tau_L = \frac{\langle L_{\text{eff}}^{(a)} \rangle}{\Delta V} \left(\frac{\Delta V}{V_0} + \gamma + \ln \kappa \right). \tag{18}$$

Finally using Eq. (13) we can get for κ the following relationship

$$\kappa = \exp\left[\Delta V \left(\frac{2\tau_L}{D} - \frac{1}{V_0} \right) - \gamma \right]. \tag{19}$$

Hence, the maximal collision number rises with (1) the decreasing diameter of nanoparticles, (2) increasing laser pulse duration, and (3) increasing the energy gained by a single collision with the boundary.

7. The maximal energy gained by FE's within τ_L

Substituting Eq. (10) and Eq. (19) with Eq. (11) into Eq. (7) one can obtain an expression for the final kinetic energy of FE's, suffering κ collisions with the boundary of the nanoparticle of diameter D exposed to laser light with wavelength λ, intensity I_L, and pulse duration τ_L

$$E_{e\text{-}h} \approx \frac{2\lambda^2 r_p I_L^{\text{eff}}}{\pi c_m} \exp\left[2\lambda \left(\frac{2\tau_L}{D} - \frac{1}{V_0} \right) \times \left(\frac{r_p I_L^{\text{eff}}}{m_{e\text{-}h}^* \pi c_m} \right)^{1/2} - \gamma \right]. \tag{20}$$

It can be easily seen from Eq. (20) that at the fixed parameters of the laser excitation (λ, I_L, τ_L) and the material used $(V_0, m_{e\text{-}h}^*, c_m, r_p)$ the energy of FE's gained by laser heating increases with decreasing nanoparticle diameter as $\exp(1/D)$. Also, the efficiency of the FE laser heating process should be much higher with increasing wavelength, intensity, and pulse duration of applied laser light.

D. Comparison with experimental data

As we mentioned above, FE laser heating leads to an increase in the FE kinetic energy. One can reach the condition at which FE's are extremely hot, so they create a high-density electron-hole plasma. The temperature of laser-heated FE's, which have suffered only a single collision with the boundary can be estimated using a gas kinetics approximation[34] as follows: $T_{\text{FE}} = (2/3)(6.4\,\text{eV}/K) \approx 0.5\,10^5\,\text{K}$, where k is the Boltzmann constant. The obtained value is typical for MP-produced excitons[38] and laser-heated plasma.[34] Because the FE's suffer many collisions, the temperature of the plasma created is expected to be much higher than the estimated value. However, the energy losses should also be taken into account in order to make a correct estimation of the maximal temperature of the electron-hole plasma. The formation of biexcitons with their subsequent transformation into Frenkel defects is assumed to be one of the pathways of FE energy relaxation. Alternatively, it has been shown experimentally that laser heating of FE's is responsible for an increase in the efficiency of the FE penetration through the STE barrier.[6] As a result, the intensity of the STEPL band becomes higher with the power of the laser light as compared to the PL bands related to the hydrogen-related centers and NBOHC's.[6]

The hot FE's reaching STE states normally lose energy by the emission of lattice phonons (the process of STE cooling).

As this takes place, the lattice is heated up to a certain temperature. Further thermal diffusion causes the cooling of nanometer-sized silica fragments. Because there is a big difference in the temperatures of electron-hole and lattice phonon subsystems, a temperature gradient is formed. One would expect that the heat transfer from hot STE's into the lattice is proportional to the temperature gradient.[14] Finally the electron-hole and lattice-phonon subsystems come to a thermal equilibrium condition, which is due to thermal losses at the boundary. If the lattice temperature at the thermal equilibrium condition is not high enough, radiative transitions can occur from the minimum of STE adiabatic potential surface into the ground state corresponding to the undisturbed lattice site (Fig. 5). However, if the lattice temperature at the thermal equilibrium condition corresponds to the energy of lattice phonons, the STE is able either to emit or absorb lattice phonons and, as a result, the radiative relaxation of STE's can involve phonon-assisted transitions (hot transitions). The availability of phonon-assisted transitions appears as additional light emission components in the STEPL band. The resulting components are situated in the short wavelength side of the STEPL band with a shift equal to the lattice phonon energy, so they form a phonon sideband. A photon emitted within this process is $\hbar\omega_{\mathrm{PL}}=E_{g_{\mathrm{STE}}}+\hbar\omega_{\mathrm{LO}}$, where $E_{g_{\mathrm{STE}}}$ denotes the STE energy gap. Accordingly, one can observe what appears to be a blue shift in the STEPL and its value will be affected by the maximal energy of FE's gained due to the laser heating process. It can be easily seen from Fig. 1 that the FWHM of the STEPL band in silica-based mesostructures slightly increases because of simultaneous contributions from phonon-free and phonon-assisted transitions. Evidently, if the more energetic phonons are involved in the emission process, the shift is greater and vice versa. The lattice temperature at thermal equilibrium condition can be estimated by using experimentally observed shifts of the STEPL bands in the same way as it has been done for heated FE's: $T_1=(2/3)(0.06\ \mathrm{eV}/K)\approx 4.6\times 10^2\ \mathrm{K}$, $T_2=(2/3)(0.15\ \mathrm{eV}/K)\approx 1.16\times 10^3\ \mathrm{K}$, $T_3=(2/3)(0.21\ \mathrm{eV}/K)\approx 1.6\times 10^3\ \mathrm{K}$. The temperatures obtained are quite reasonable.

Let us consider now what kinds of SiO_2 lattice phonons can be involved in phonon-assisted transitions. According to Ref. 36, there exist three types of LO (longitudinal-optical) and TO (transverse-optical) phonon modes in silica nanoparticles, which correspond to three different local vibrational motions of oxygens with respect to the silicon atoms: the rocking, bending, and asymmetrical motions, respectively. The corresponding frequencies are the following: $\mathrm{TO}_1=424\ \mathrm{cm}^{-1}\ (0.053\ \mathrm{eV})$, $\mathrm{LO}_1=471\ \mathrm{cm}^{-1}\ (0.058\ \mathrm{eV})$, $\mathrm{TO}_2=791\ \mathrm{cm}^{-1}\ (0.098\ \mathrm{eV})$, $\mathrm{LO}_2=1005\ \mathrm{cm}^{-1}\ (0.125\ \mathrm{eV})$, $\mathrm{TO}_3=1086\ \mathrm{cm}^{-1}\ (0.135\ \mathrm{eV})$, $\mathrm{LO}_3=1206\ \mathrm{cm}^{-1}\ (0.150\ \mathrm{eV})$. As we demonstrated above, the STEPL blue shift for 15 nm particles is 0.06 eV, so this can be attributed to the activation of LO_1 phonon-assisted transitions (Fig. 5). The more energetic phonons are involved in the case of 7 nm silica nanoparticles in full agreement with the theoretical prediction. Accordingly, the radiative transitions are assisted by a combined phonon mode $\mathrm{LO}_1+\mathrm{LO}_3$ $(0.058+0.15=0.208\ \mathrm{eV})$, the energy of which is close to the experimentally observed blue shift (0.21 eV) (Fig. 5).

The STEPL blue shifts observed in mesoporous silicas can be interpreted in the same way. First note that the FE laser heating model completely eliminates the contradiction mentioned in Sec. B. It becomes evident that in the case of small-radius Frenkel excitons the wall thickness in the range of $\sim$1 nm is large enough to expect the QC effect. On the other hand, because the materials possess a regular array of uniform channels, the walls can be considered as one-dimensional silica fragments with $\sim$1 nm width. One can imagine that the FE's are able to move along the one-dimensional fragments without collisions with the boundary thus hampering laser heating. As a result, the blue shifts observed in the mesoporous silicas are smaller than those in 7 nm silica nanoparticles. Also, the ordering of mesoporous materials affects the heating efficiency. Since the disordered mesoporous silicas contain many defects in the regularity of channels and since this feature will lead to the high incidence of FE collisions, it is reasonable to assume that the laser-heating efficiency should be somewhat higher than that in ordered materials. This is a reason why the blue shift for STEPL band in MCM-41 materials does not occur. Accordingly, the 0.06 eV blue shift in the 2 nm pore sized disordered mesoporous silica is assumed to be due to an activation of LO_1 phonon-assisted transitions, similarly as for 15 nm silica nanoparticles. In the case of 6 nm pore sized material the activation of LO_1 and LO_3 phonon-assisted transitions are responsible for the 0.06 and 0.15 eV shifts, respectively. The greater blue shift for 6 nm pore sized materials indicates that the heating efficiency of FE's in this case is higher than that for smaller pore sized mesoporous silica. This means that the collision number of FE's with the boundary is greater and in turn the wall thickness among mesopores is expected to be thinner.

It should be noted that the blue shift of the STEPL band in the model presented is determined both by the maximal energy of FE's gained by laser heating before being self-trapped and by a combination of phonon modes existing in the given kind of materials at the lattice temperature corresponding to the thermal equilibrium condition between electron-hole and lattice-phonon subsystems. It has been shown above that the maximal energy of FE's increases with decreasing size of nanoparticles as a function of $\exp(1/D)$ [Eq. (20)]. Because of the proportionality between the heat transfer rate and the temperature gradient mentioned above, the final lattice temperature at the thermal equilibrium condition will be proportional to the maximal temperature of laser-heated FE's. Therefore, the function $\exp(1/D)$ can be applied to describe the dependence of the STEPL band shift with decreasing size of silica fragments. Of course, the fit to experimental data is somewhat qualitative because of the simplified type of the fitting function and the fact that the actual size of nanoparticles allows for some variations. However, we discuss here the essential physics of the process. Our task is to identify the physical mechanisms responsible for the observed blue shift in the excitonic PL for wide-band-gap nanoscale materials. From this point of view, the func-

tion exp(1/D) that arises from the new model correctly describes a tendency for the shift of the STEPL band in silica nanomaterials. Since the properties of the function exp(1/D) is close to that of $1/D^2$, the blue shift of STEPL band can be fitted by either of them (Fig. 3), despite the fact that $1/D^2$ function is usually consistent with the QC effect but exp(1/D) is related to the FE laser heating process. The similarity of the function types, describing the blue shift of excitonic PL with decreasing size of nanometer-sized fragments, may be a source of errors in the interpretation of size effects on excitons in wide-band-gap nanoscale materials.

Alternatively to the hot radiative transitions mentioned above, it is reasonable to expect a similar phonon-assisted process in the absorption of light by solids. Accordingly, the phonon emission accompanying the light absorption process (an indirect process) should manifest itself as a shift in the excitonic absorption band. Such type of indirect transitions was observed in photoelectron emission from the bulk diamond due to exciton breakup.[39] Taking into account the phonon-assisted transition conception let us consider the experimental results taken from the x-ray-absorption spectroscopy of nanodiamonds, initially explained as a QC effect on the core exciton.[9] First note that the authors of the paper quote the QC effect on Mott-Wannier excitons in Si nanocrystals[3,40] as similar to the situation occurring in nanodiamonds. However, the nature of excitons in bulk diamond and silicon is completely different. As mentioned in the Introduction, the effective bohr radius of the core exciton in diamond is 0.17 nm,[13] whereas it is estimated to be ~5.25 nm in silicon.[41] Additionally, the Mott-Wannier exciton in silicon is an example of the weak vibronic coupling effect,[41] whereas the core exciton in diamond is characterized by a very strong vibronic coupling constant, resulting in the appearance of a phonon sideband in x-ray emission spectra with vibrational numbers as high as 35.[10] It is evident from this comparison that the size effect in these nanocrystals cannot be considered jointly. Despite this fact the authors of Ref. 9 used the QC model developed for Mott-Wannier excitons in semiconductors. Moreover, they pointed to a monotonic shift of excitonic peak in the C K-edge absorption spectrum towards higher energies as a crystallite radius decreases. However, it can be easily seen from the corresponding figure that the peak practically does not shift (289.0 eV) for crystallites with radii in the range of 35 nm to 5 μm, whereas it is situated at 289.4 eV when the size is less than 35 nm (27–3.6 nm). Because of indirect band-gap and strong vibronic coupling effect for diamond,[10,39] the aforementioned blue shift can be explained in the framework of the many-body dynamics discussed in Ref. 39, as an activation of TO phonon (0.16 eV)-assisted transitions rather than the QC effect on core excitons. The emission of two or three TO phonons is already enough to cover the blue shift range observed in Ref. 9. Note finally that the explanation suggested is based on the generally accepted notions of modern solid-state physics[14,15] and does not require any additional assumptions.

IV. CONCLUSIONS

In summary, we have provided evidence for a size effect in STEPL from SiO_2-based nanoscale materials. The STEPL blue shift with decreasing size of nanometer-sized silica fragments in mesostructures studied has been treated by two models taking into account the QC effect and FE laser heating by a strong electromagnetic field. We have showed that the use of the QC model developed for the Mott-Wannier excitons in semiconductor nanoscale materials is totally unsuited for Frenkel excitons typically existing in wide-band-gap materials. Alternatively, our model, which is based on the conception of the FE laser heating gives good agreement with experimental data. We suggest that the blue shift of the STEPL band originates from the activation of phonon-assisted transitions. The greater blue shift corresponds to the activation of hot transitions involving more energetic phonons or their combination. The blue shift of the STEPL band depends on the temperature of laser heated FE's that in turn is determined by the size of nanometer-sized silica fragments. This happens because the temperature (kinetic energy) of the laser-heated FE increases with the number of collisions with the boundary of confined regions, which tends to be higher with decreasing size of silica fragments in nanoscale materials. The model proposed in this paper shows that the blue shift of PL bands in nanoscale materials in general does not need to be related always to a QC effect.

ACKNOWLEDGMENTS

The authors acknowledge Academia Sinica and China Petroleum Corporation of Taiwan, Republic of China, for financial support. The work also was supported by National Science Council of Taiwan: Y.D.G. and S.H.L. Grant No. 89-2113-M-001-050, L.P.H. Grant No. 89-2113-M-002-033, and Y.T.C. Grant No. 89-2113-M-001-032.

*Corresponding author: Email address: yuri.d.glinka @vanderbilt.edu; Permanent address: Institute of Surface Chemistry of the National Academy of Sciences of Ukraine, Prospekt Nauki 31, Kiev 252650, Ukraine.

[1] *Nanomaterials: Synthesis, Properties, and Applications*, edited by A. S. Edelstein and R. C. Cammarata (Institute of Physics Publishing, Bristol, U.K., 1996).

[2] J. P. Proot, C. Delerue, and G. Allan, Appl. Phys. Lett. **61**, 1948 (1992).

[3] S. Ogut, J. R. Chelikowsky, and S. G. Louie, Phys. Rev. Lett. **79**, 1770 (1997).

[4] Al. L. Efros and A. L. Efros, Fiz. Tekh. Poluprovodn. **16**, 1209 (1982) [Sov. Phys. Semicond. **16**, 772 (1982)].

[5] L. E. Brus, J. Chem. Phys. **79**, 5566 (1983).

[6] Yu. D. Glinka, S. H. Lin, and Y.-T. Chen, Phys. Rev. B **62**, 4733 (2000).

[7] Yu. D. Glinka, S. H. Lin, L. P. Hwang, and Y.-T. Chen, J. Phys. Chem. B **104**, 8652 (2000).

[8] A. N. Trukhin, J. Non-Cryst. Solids **149**, 32 (1992).

[9] Y. K. Chang, H. H. Hsieh, W. F. Pong, M.-H. Tsai, F. Z. Chien, P. K. Tseng, L. C. Chen, T. Y. Wang, K. H. Chen, D. M. Bhusari, J. R. Yang, and S. T. Lin, Phys. Rev. Lett. **82**, 5377 (1999).

[10] Y. Ma, P. Skytt, N. Wassdahl, P. Glans, D. C. Mancini, J. Guo, and J. Nordgren, Phys. Rev. Lett. **71**, 3725 (1993).
[11] E. I. Rashba, in *Excitons; Selected Chapters*, edited by E. I. Rashba and M. D. Sturge (Elsevier, Amsterdam, 1987), p. 273.
[12] P. E. Batson, Phys. Rev. Lett. **70**, 1822 (1993).
[13] F. Mauri and R. Car, Phys. Rev. Lett. **75**, 3166 (1995).
[14] O. Madelung, *Introduction to Solid-State Theory* (Springer-Verlag, Berlin, New York, 1978).
[15] C. Kittel, *Introduction to Solid State Physics* (Wiley, New York, 1986).
[16] D. L. Griscom, in *Proceedings of the Thirty-Third Frequency Control Symposium* (Electronics Industries Assn., Washington, DC, 1979), p. 98.
[17] C. Itoh, K. Tanimura, N. Itoh, and M. Itoh, Phys. Rev. B **39**, 11 183 (1989).
[18] W. Joosen, S. Guizard, P. Martin, G. Petite, P. Agostini, A. Dos Santos, G. Grillon, D. Hulin, A. Migus, and A. Antonetti, Appl. Phys. Lett. **61**, 2260 (1992).
[19] Yu. D. Glinka, S. N. Naumenko, and V. Ya. Degoda, J. Non-Cryst. Solids **152**, 219 (1993).
[20] K. Arai, H. Imai, H. Hosono, Y. Abe, and H. Imagawa, Appl. Phys. Lett. **53**, 1891 (1988).
[21] T. E. Tsai and D. L. Griscom, Phys. Rev. Lett. **67**, 2517 (1991).
[22] C. T. Kresge, M. E. Leonowicz, W. J. Roth, J. C. Vartuli, and J. S. Beck, Nature (London) **359**, 710 (1992).
[23] Yu. D. Glinka, S. H. Lin, and Y.-T. Chen, Appl. Phys. Lett. **75**, 778 (1999).
[24] N. Kuzuu, Y. Matsumoto, and M. Murahara, Phys. Rev. B **48**, 6952 (1993).
[25] R. Schmidt, E. W. Hansen, M. Stocker, D. Akporiaye, and O. H. Ellestad, J. Am. Chem. Soc. **117**, 4049 (1995).
[26] N. Ulagappan and C. N. R. Rao, Chem. Commun. (Cambridge) **24**, 2759 (1996).
[27] A. Monnier, F. Schuth, Q. Huo, D. Kumar, D. Margolese, R. S. Maxwell, G. D. Stucky, M. Krishnamurty, P. Retroff, A. Firouzi, M. Janicke, and B. F. Chmelka, Science **261**, 1299 (1993).
[28] D. L. Griscom, J. Ceram. Soc. Jpn. **99**, 923 (1991).
[29] L. Skuja, J. Non-Cryst. Solids **179**, 51 (1994).
[30] I. T. Godmanis, A. T. Trukhin, and K. Hubner, Phys. Status Solidi B **116**, 279 (1983).
[31] Y. R. Shen, *The Principles of Nonlinear Optics* (Wiley, New York, 1984).
[32] F. B. Bunkin, A. E. Kazakov, and M. V. Fedorov, Sov. Phys. Usp. **15**, 416 (1973).
[33] N. M. Kroll and K. M. Watson, Phys. Rev. A **8**, 804 (1973).
[34] N. I. Koroteev and I. L. Shumay, *Physics of High-Power Laser Radiation* (Nauka Publishers, Moscow, 1991) (in Russian).
[35] Yu. D. Glinka and M. Jaroniec, Phys. Rev. A **56**, 3056 (1997).
[36] Yu. D. Glinka and M. Jaroniec, J. Appl. Phys. **82**, 3499 (1997).
[37] A. Jeffrey, *Handbook of Mathematical Formulas and Integrals* (Academic, New York, 1995).
[38] Yu. D. Glinka, K.-W. Lin, H.-C. Chang, and S. H. Lin, J. Phys. Chem. B **103**, 4251 (1999).
[39] C. Bandis and B. B. Pate, Phys. Rev. Lett. **74**, 777 (1995).
[40] N. A. Hill and K. B. Whaley, Phys. Rev. Lett. **75**, 1130 (1995).
[41] V. B. Timofeev, in *Excitons Selected Chapters*, edited by E. I. Rashba and M. D. Sturge (Elsevier, Amsterdam, 1987), p. 229.